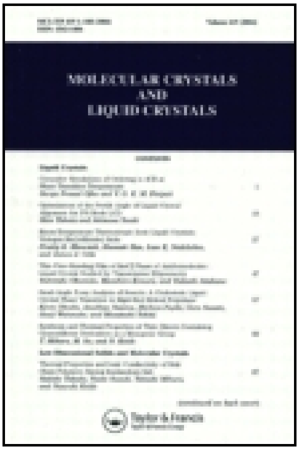

Molecular Crystals and Liquid Crystals Science and Technology. Section A. Molecular Crystals and Liquid Crystals

Publication details, including instructions for authors and subscription information:
http://www.tandfonline.com/loi/gmcl19

AFM on Chemically Reacting Crystals

Gerd Kaupp [a]

[a] University of Oldenburg, FB 9 - Organische Chemie I, P. O. Box 2503, D-26111, Oldenburg, Germany

Version of record first published: 24 Sep 2006.

To cite this article: Gerd Kaupp (1994): AFM on Chemically Reacting Crystals, Molecular Crystals and Liquid Crystals Science and Technology. Section A. Molecular Crystals and Liquid Crystals, 242:1, 153-169

To link to this article: http://dx.doi.org/10.1080/10587259408037748

Mol. Cryst. Liq. Cryst. 1994, Vol. 242, pp. 153–169
Reprints available directly from the publisher
Photocopying permitted by license only

Printed in the United States of America

AFM ON CHEMICALLY REACTING CRYSTALS

GERD KAUPP
University of Oldenburg, FB 9 - Organische Chemie I -
P.O.Box 2503, D-26111 Oldenburg, Germany

Abstract A review is given on recent developments of atomic force microscopic (AFM) studies on chemically reacting organic crystals. Three further basic phase transformation mechanisms have been added to the previous five. Both photodimerizations and gas/solid reactions are studied in detail by scanning the surfaces of initial and chemically reacted crystals of anthracenes, thiohydantoines, α- and β-cinnamic acid, and stilbene at different faces, where technically possible. The AFM-features are correlated to known crystal structure data with the aid of semiempirical calculations in part. Thus, detailed molecular mechanisms for the far-reaching well-directed transport phenomena may be derived in most cases and the appearance of the submicroscopic features rationalized. Unimolecular terrace steps of anthracene behave as independent crystal face already. The addition of bromine and chlorine leads to new solid phases directly even though there might be formed mixtures of stereoisomers. If a submicroscopic liquid phase is formed as in the reaction of α-cinnamic acid with chlorine, the surface will be remodelled by the tip and this provides for interesting nanostructures. In many cases there are secondary phase transformations apparently from one form of mixed crystals into another form of mixed crystals either upon continuation of irradiation or just on standing of gas/solid reacted crystals for several hours.

Keywords atomic force microscopy, solid state photochemistry, gas/solid reaction, basic mechanism, phase transformation, molecular mechanism, unimolecular step, crystal face, crystal structure, nanostructures

INTRODUCTION

Atomic force microscopy (AFM) turned out to be a versatile new tool for mechanistic studies in solid state chemistry. This has been shown in photolyses of crystals and in gas/

solid reactions.[1-5] Following the initial collection of empirical data in this totally unprecedented field of research many efforts have been made in explaining the observed features on a molecular basis by correlations with crystal structures and molecular geometries. This proved to be an important goal, because the well-directed and far-reaching transport phenomena were completely unforeseen and they point to realistic rationalizations of topochemically forbidden and topochemically allowed but not proceeding reactions on a sound experimental basis. Also an understanding of the hitherto unexplainable gas/solid reactivity could be achieved on account of the availability of now eight different basic phase transformation mechanisms. It turns out that crystal structure is much more intimately related to solid state reactivity than has been assumed by the topochemical principle, but the new powerful experimental technique AFM shows that there are also further effects at work.

EXPERIMENTAL

A Digital Instruments NanoScope II/5 was used with commercial Si_3N_4 cantilevers and tips.[1-5] For colour imaging NanoScope III software was used in connection with a Mitsubishi Videoprinter CP-200E (H). These were photographed for glossy black and white prints. Crystal packing drawings were generated from published X-ray data by using SCHAKAL92 (AIX-UNIX version, E. Keller, Universitaet Freiburg) at an IBM RS 6000 32H workstation. Van der Waals surfaces are semiempirically calculated (MOPAC, PM3) and plotted with PCMODEL of QCPE. Single crystals were obtained as described.[1] 3 was crystallized from ether. Irradiations were performed directly on the AFM stage from 5 cm distance with a Hanau 150 W Hg-high pressure lamp through a water-cooled Solidex filter.[1,3-5] The application of gases after removal of the head was with a 1 ml syringe from about 1 cm distance which was pushed out in about 5 s. Then the environment of the whole AFM stage was flushed with Ar in order to remove Cl_2 or Br_2 which would destroy the gold coating of the cantilever. First measurements were routinely obtained 10 min after gas applications. Possible hydrolysis effects were excluded by control experiments via keeping gas-treated crystals for 20 h in vacuum and looking for the same features as in the experiments in normal atmosphere.

BASIC MECHANISMS

According to previous AFM studies (non-topotactical) solid state reactions are governed by their phase transformation mechanisms. There could be added three further basic mechanisms to the previously known five.[4] These are the formation of floes,[1] islands,[2] and eggs' pallets.[3] Representative examples are shown in Figure 1 and Figure 4 below.

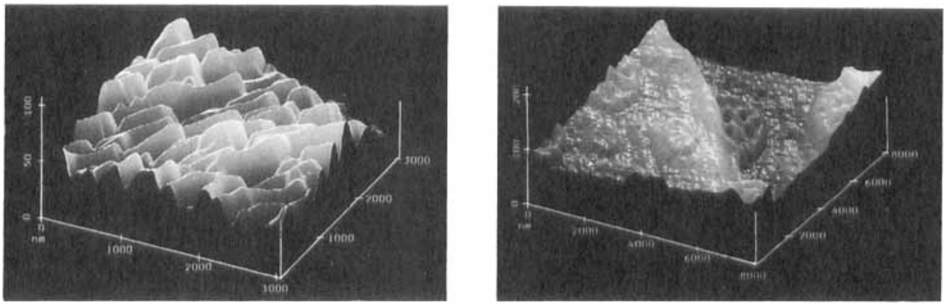

FIGURE 1 Floes from photolysis of 9-chloroanthracene[1] and islands from gas/solid reaction of 3-phenylthiohydantoin with CH_3NH_2[2]

In Figure 1 it can be seen how evenly such floes may be formed, and on the right hand side the different stages of island formation as well as an artificially sliced island are easily observed within one AFM scan.

All of the eight basic mechanisms appear to correlate well with the initial crystal structures of the starting materials.[1-3,5] Most convincing appears the explanation of the crater formation in the initial stages of the photolysis of ß-cinnamic acid ($P2_1/a$) on (100) in Figure 2.[1b] The molecules cut (100) at an angle of 83°. If the photodimer (ß-truxinic acid) is formed, it may rotate as indicated by 90° and 60° in order to geometrically fit into the host lattice. However, the dimer has shrinked by about 30 % with respect to 2 molecules of cinnamic acid (1). As this horizontal shrinking is faster in the upper layers where more light is absorbed and slower in the deeper layers, the observed craters must be formed. Their width is 500 nm, their depth 200 nm. The obvious upward transport is caused by the breaking of hydrogen bonds upon dimerization and the complete leveling out of all crater structure upon further

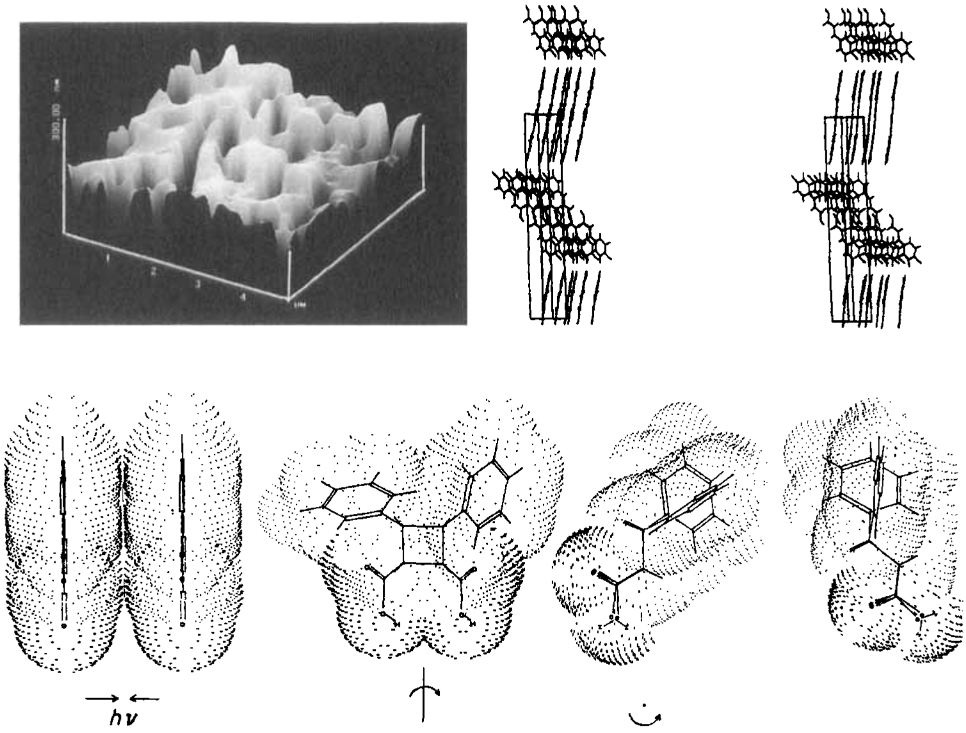

FIGURE 2 Top left: AFM scan of craters formed all over upon short irradiation of ß-1 on (100). Top right: Stereoview of model crystal structure 4-chlorocinnamic acid. Bottom: PM3-surfaces of 1 and its photodimer indicating its fit in.

irradiation[1,5] is apparently caused by a thermal phase transformation of mixed crystals which are rich in starting material into mixed crystals which are rich in product. The reason for this is the necessity to maximize the number of hydrogen bridges.[5]

PHOTOLYSIS OF ANTHRACENE

It has been repeatedly shown[1a,4,5] that there are no thermal effects upon normal irradiations with Solidex-filtered high-pressure lamps down to the molecular level. Therefore we can study the photochemical behaviour of unimolecular and oligomolecular terrace steps upon photolysis of the face which carries such terraces. It is very easy to distinguish mono-, bi-, tri-, and tetramolecular steps on the (001) face of anthracene which are 10, 20, 30, and 40 Å high (Figure 3, left).

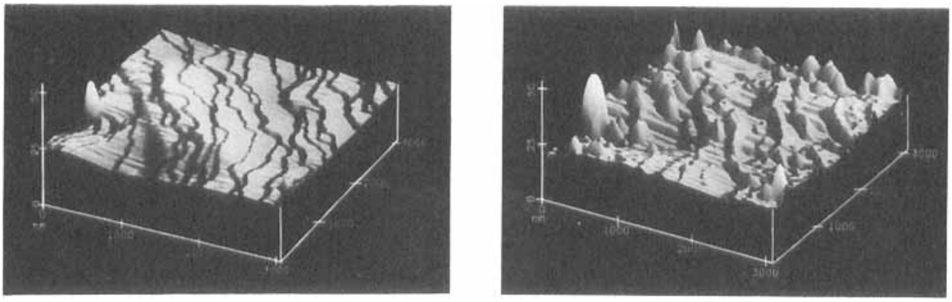

FIGURE 3 AFM surfaces; left: molecular steps on (001) of anthracene; right: dimer formation after 1 min irradiation[1]

It is well known that crystalline anthracene gives its photodimer upon photolysis, even though such reaction is topochemically forbidden. On the right hand side of Figure 3 the very early stage of this reaction shows that the new features grow along those molecular steps and even along the unimolecular ones (light penetration depth at $\lambda = 365$nm around 200 nm). Thus, there are far-reaching transport phenomena and we are in the phantastic situation that even a monomolecular step behaves as an independent crystal face which is closed on one side. This is an important clue to any defect or disorder discussion which will have to be put down to the unimolecular level from now on. The crystal structure of anthracene[6] allows for a molecular interpretation which indicates its considerably more intimate relation to reactivity than any version of topochemical principle. It has been shown[1b] that anthracene molecules cut (001) ($P2_1/a$) at an angle of 67° and form parallel layers of 10 Å thickness. From this knowledge it is quite clear that the steep molecules at the molecular steps may be easily pushed away as there is formed internal pressure by photodimerization at the site of light absorption within the layers. Thus, material is forced out at the molecular steps and builds up the chainy hills along the steps. Also pressure built up in the lower layers will be released via upward and sideward transport through the steps, because the hills grow up to 50 nm height in later stages of the irradiation, prior to the final phase transformation into floes.[1] A similar behaviour is found for 9-cyanoanthracene (steps on (010)), whereas 9-chloro- and 9-methylanthracene react uniformly all over their morphologically dominant faces.[1] An example is shown in Figure 1 (the long sideface of 9-chloroanthracene gives beautiful volcanoes).[1] In gas/solid reactions there is also a system known where the extended face gives different reaction features than at a 9 nm step on it with 27 molecular layers.[2]

GAS/SOLID REACTIONS WITH CINNAMIC ACID

The addition of gaseous bromine to cinnamic acid **1** has been known since 1863.[7] We could show by ^{1}H-NMR that both α- and β-cinnamic acid yield the erythro isomer **2** (X = Br) exclusively ($J_{2H/3H}$ = 11.7 Hz). The reaction of chlorine with 1 gives partial liquefaction after 2 - 3 h at room temperature. As chlorine dissolves readily in this liquid, the reaction may continue in this case up to completion. It provides threo- ($J_{2H/3H}$ = 7.3 Hz) and erythro-2 (X = Cl) ($J_{2H/3H}$ = 11.0 Hz) in 88 and 12 % yield. A similar ratio (91 : 9) is found at -20°C and there is slow liquefaction under 0.4 to 0.8 bar of chlorine. Thus, an initial gas/solid reaction becomes a gas/liquid reaction in this case.

The AFM-studies of these reactions are quite rewarding and show an intimate relation of crystal structure and phase transformation mechanism. If Br_2 reacts with α-cinnamic acid (α-1) there are formed both 200 nm deep craters and 200 nm high volcanoes with some pillars on the initial (010) face. This looks pretty much like an eggs' pallet

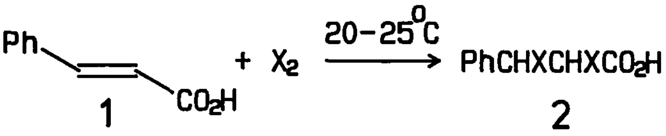

α or β , X_2=Br_2: erythro-2 (R=Br)

α or β , X_2=Cl_2: threo/erythro = 88:12 (liquefies)

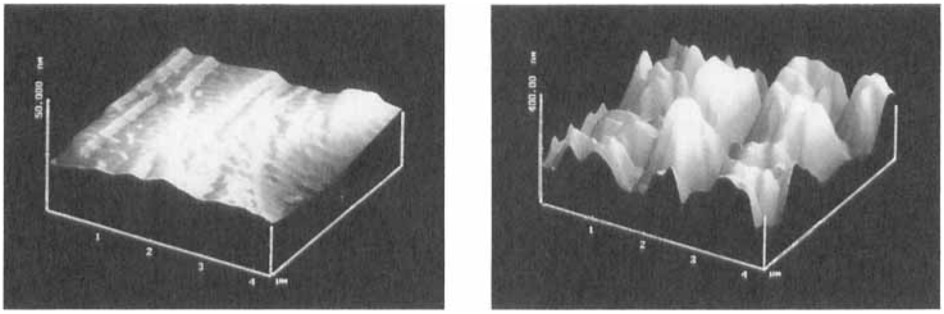

FIGURE 4 AFM surface of α-1 ($P2_1/n$) (010) (left) and after exposure to bromine vapor (right)

and should be termed a separate phase transformation mechanism. It appears obvious that the arrangement of molecules

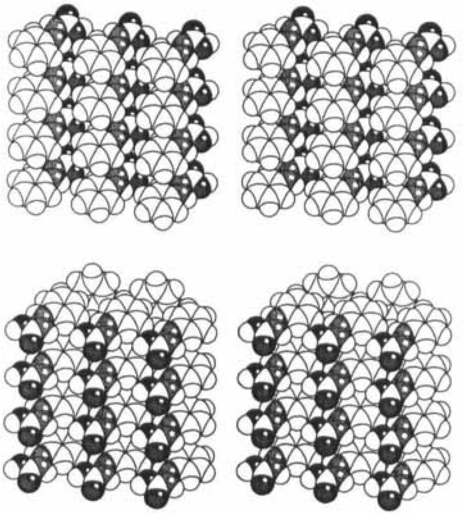

FIGURE 5 Stereoscopic view of the molecular packing facing (010) of α-**1** in the two different alternating layers parallel to (010); double bond-C with circles, O with mesh

at the surface should be important for the molecular mechanism of the far-reaching transport processes observed. It can be seen in Figure 5 that the double bond of flat lying (30°) α-**1** is relatively accessible from one side in one of the layers, whereas it is shielded by the phenyl groups in the other. It is intelligible that the usual bromonium ion may form easily in the bottom type layers. As the product structure **2** (X = Br) is erythro, there must be a trans-addition. However, the second bromine atom (formally bromide anion) cannot attack the three-membered bromonium ion from the backside unless this has considerably moved out of the layer. Thus, there must be an upward transport and molecules from the differently oriented layer below may only partially move in to fill the gap. If all of the bottom type layer has reacted, bromine gas will have to penetrate below the next layer for further reaction from below the surface and the neighbouring molecules will have to glide upward in order to provide space for completion of the addition. In this situation both volcanoes and craters form nucleation centers (the pillars) in a very regular way as dictated by the crystal structure.

If β-1 ($P2_1/a$) is exposed to Br_2 gas on (100) reaction zones are moving over the crystal, whereas on (010) there is more uniform formation of rather flat floes which transform into more pronounced features upon standing for 20 h presumably because of a phase transformation. Thus, again there is a completely different behaviour on different faces of β-1 which must directly correlate with crystal structure. As the crystal structure of β-1 is still not known, 4-chlorocinnamic acid provides the closely related

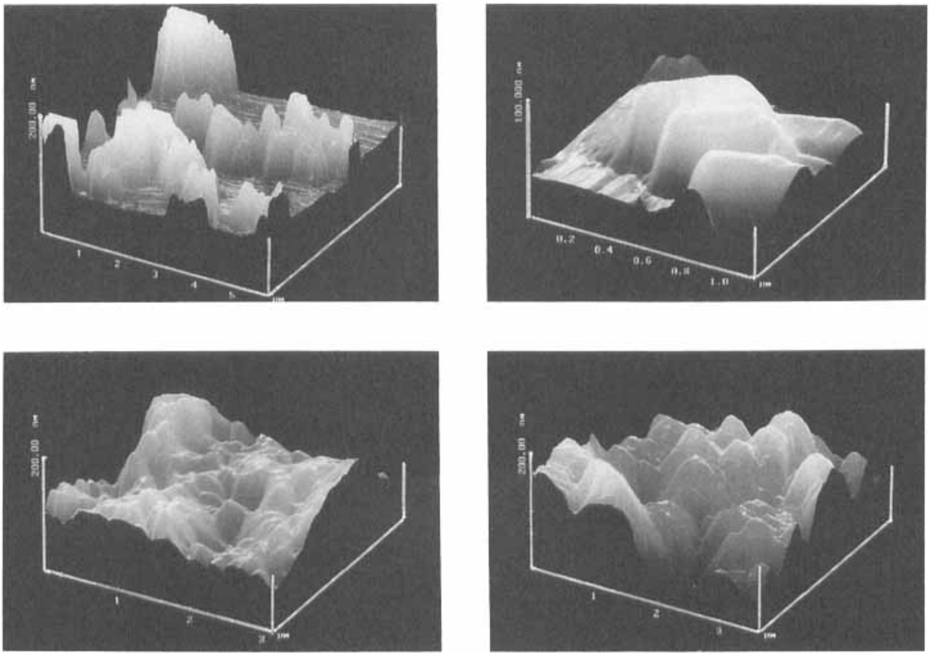

FIGURE 6 AFM surfaces of β-1 after exposure to bromine; top, promptly on initial (100); bottom on initial (010), left promptly measured, right after 20 h standing

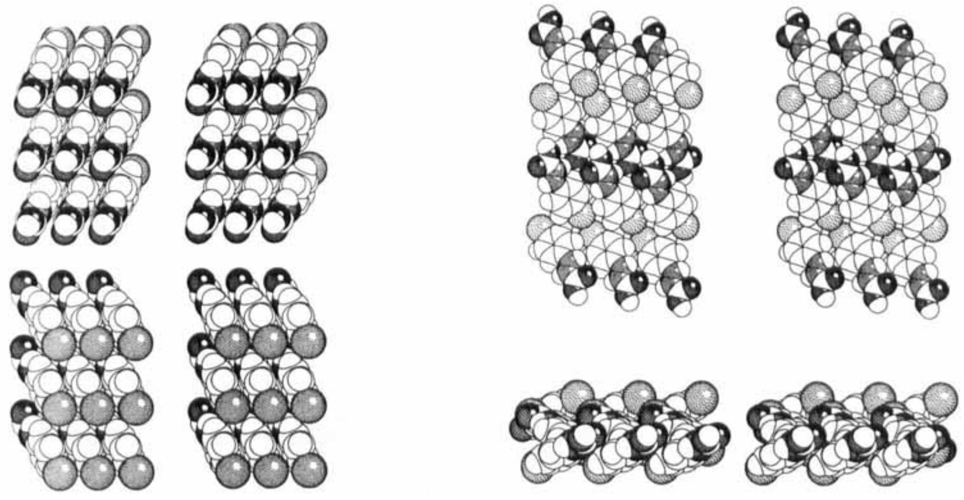

FIGURE 7 Stereoscopic views of the molecular packing facing (100) (left) and (010) (right) of β-1; at the bottom right diagram (010) is on top; double bond C with circles, O with mesh, Cl with dotted circles

model structure.[8] It is easily seen from Figure 7 left that both of the alternating layers have the molecules very steep (83°) on (100). The double bonds are shielded by the carboxyls in the top and even more so by the aryl groups in the bottom layer of Figure 7. They appear inaccessible. Therefore, for a reaction with bromine to occur the molecules must come out straight upward. Once started, this gliding upward will continue zonally from the nucleation centers, because all molecules are parallel and not interlocked. This is completely different from α-1, where the molecules lie relatively flat. One notes from the larger magnification in Figure 6, that the buildup of the sharply edged features involves trenches. Thus, the reacting zone eats itself into the surface region of the crystal.

On (010) of β-1 the situation appears rather easy. One half of the double bonds lies easily accessible and flat (23°) on the surface (Figure 7). There should be no problem for initially formed bromonium ions to turn around for backside attack and thus, there appear no problems for nucleation. The second half of the molecules will gain enough mobility after reaction of their neighbours and a relatively featureless floe formation occurs. These features become somewhat more structured upon standing. This is probably the result of a thermal phase transformation, as there are no signs of hydrolysis detectable (neither on (100) of ß-1, where the structures stay sharp upon standing in air).

There might be some concern about short-lived liquid phases on the molecular level, but this will inevitably run into problems of definition (where does a solid phase start to become a liquid phase if only a few molecules are considered?). However, AFM is able to detect genuine liquid phases: If a viscid phase is formed, the tip will stick to it and the cantilever will considerably bend or eventually break if it is tried to snap the tip free. Under these conditions no AFM-measurements are possible in contact mode. If a highly viscous liquid phase is formed, the tip spreads it along the scan direction (see Figure 5b in Ref. 4) and it will stay there for some time. If, however, a liquid of relatively low viscosity is formed as in the reaction of 1 with Cl_2, there will be gradual remodelling of the surface upon continuous AFM-scanning. The liquid dissolves some of the crystalline material and this solution is transported back and forth with the easily immersing tip.

Figure 8 shows a rather rough portion (mean roughness 5.4 nm) of a (010) face of α-1 (if compared to Figure 4, where a crystal of a different crop was used) and a hole generated by short exposure to chlorine and 26 min scanning. It is seen that the bottom of the hole is flat and that there are piles of solid material to the left and to the right of the clearly tip generated hole. It is of great interest to follow the generation of such holes. This is done in the bottom part of Figure 8 with top-views of the starting surface, the first image after exposure to chlo-

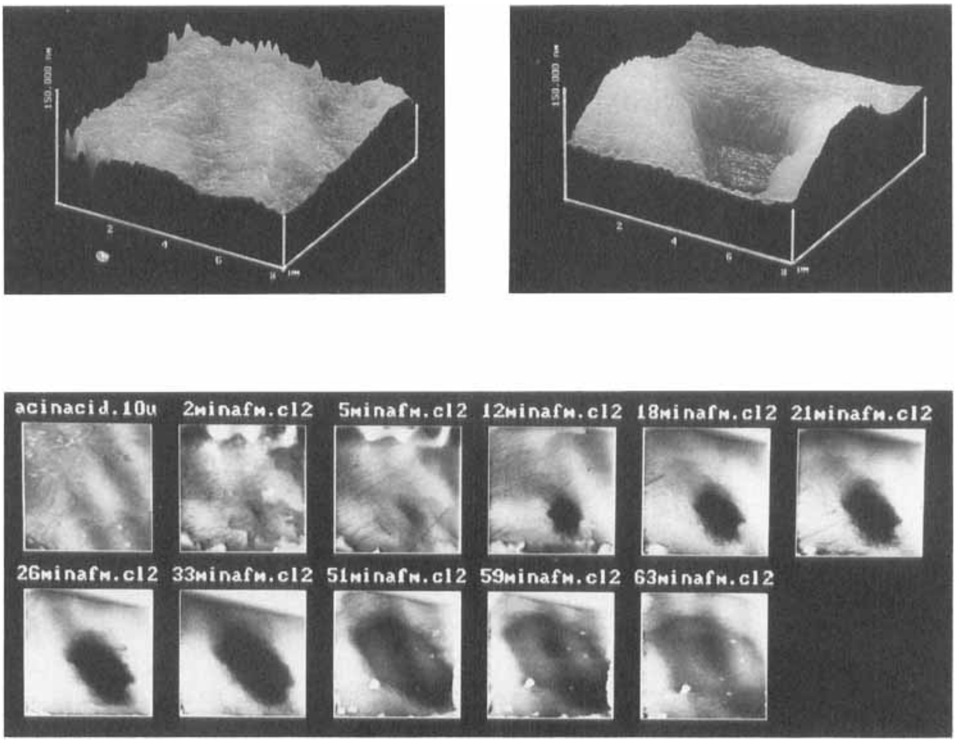

FIGURE 8 AFM surfaces of α-1 on (010) zoomed from 10 µ scans before (upper left) and after exposure to chlorine and 26 min scanning (upper right) as well as top-views of the development of the tip-generated hole in 10 µ scans; the white bars in the upper parts of some of the top-views are caused by obstacles which were formed outside the scan region

rine and remounting of the scanner, and various scans after the times given. It is seen that there is a little hole after two minutes (40 nm deep) which continually increases (maximum depth 113 nm after 12 min) in width, while there is piling of solid material to the left and to the right (light spots). At 51 min it is seen that a new hole develops at the flat bottom of the now very huge hole which continues to grow and there is also formation of stable peaks (white spots) starting at 33 min, presumably by crystallization of one of the constituents. Also at the turn of the tip there is deposition of material, of course. Thus, liquid phases, if formed upon solid state reaction, are easily recognized by AFM. They may be used to mechanically restructure the geometry of the surface while generating nanostructures. The mediating submicroliquid of apparently low viscosity is not seen by AFM in contact mode.

GAS/SOLID REACTIONS WITH STILBENE

The composition of the products from the addition of gaseous bromine and chlorine to crystalline trans-stilbene[9] has been redetermined recently.[10] It has been shown, that both the meso- and the racem-adducts (formally trans- and cis-addition) are obtained and that there is almost no aromatic substitution in the absence of acid.[10] With bromine there is prevalence of trans-addition, with chlorine the cis-addition predominates as in the case of 1. This behaviour shows that it is not only the crystal structure that determines the reaction, but also the reactivity of the gas and the reaction mechanism play their roles. It is highly indicative that bromonium ions should have more weight than chloronium ions in the well accepted addition mechanisms.

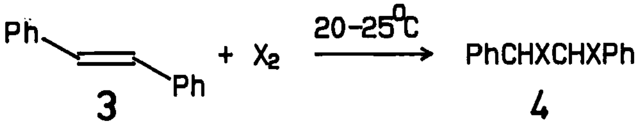

3 , X_2=Br_2 : **4** (X=Br), meso/racem=62: 38

3 , X_2=Cl_2 : **4** (X=Cl), meso/racem=39: 61

It is important to realize that completely different phase transformation mechanisms apply. Thus in the reaction of Cl_2 on the slightly structured (001)-surface (terrace heights: 16 Å = 2 molecular layers) there is found the flat cover mechanism[4], which puts a smooth blanket all over,

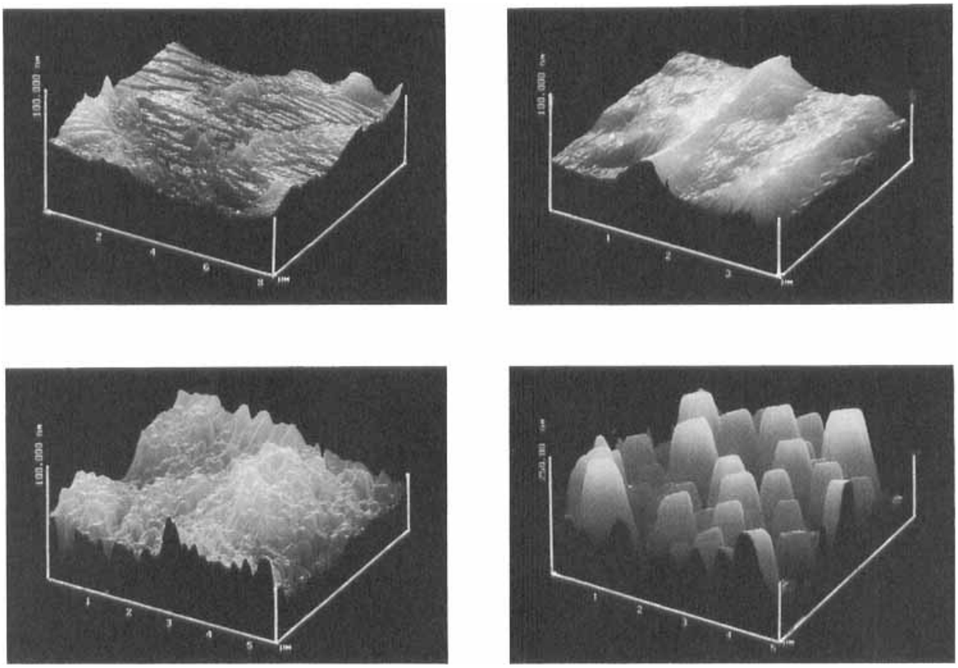

FIGURE 9 AFM surfaces of **3** (001) ($P2_1/a$)[11] before (top left) and after exposure to chlorine (top right); reaction of **3** with bromine measured promptly and after 1 day's standing (bottom left and right)

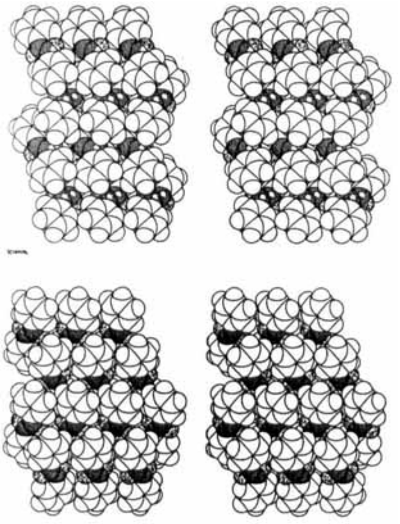

FIGURE 10 Stereoscopic views of the molecular packing of the alternating layers of **3** on (001)

whereas the bromine addition leads to craters initially. However, the situation of Figure 9 bottom left is a metastable one. Upon standing (without further addition of Br_2) smooth hills grow up (not shown) which keep growing and collapsing to the very regular 250 nm high flat plugs within 20 h. These very regular nanostructures are the result of a thermal phase transformation.

Due to the complexity of the system, there will be no exhaustive molecular interpretation of the features of Figure 9. However, the packing diagrams of 3 (Figure 10) provide important hints even though there appears to be much disorder in the stilbene crystals,[11] and even though there are three products 4 formed roughly in a ratio of 3 : 3 : 4 with Cl_2 and 6 : 2 : 2 with Br_2 (phase diagrams are not known). The layers of 3 differ slightly in the steepness of the molecules on (001) which is 39° for the top and 43° for the bottom layer of Figure 10. All molecules are strongly interlocked and the double bonds are not accessible for attack of Cl_2 or Br_2 on that face unless the lattice is broken up by molecules gliding upward out of the lattice (the situation at the bimolecular steps in Figure 9 could not be studied with the present technic of gas application, because the reactions are too fast). The coming up of molecules is clearly indicated by crater formation in both cases. Apparently it will be easier for the gas to approach the double bonds of 3 at the crater walls formed. The products 4 are pushed upward and spread horizontally on top in the reaction of chlorine (Figure 9, top right), but also in the Br_2 reaction initially (Figure 9, bottom left; there is no eggs' pallet appearance as in Figure 4). In the case of Br_2 there continues a thermal phase transformation to form the vertical features (flat plugs as shown in Figure 9, bottom right). Thus, even here the crystal structure influences the features observed and helps in rationalization of the experimental results.

CONCLUSIONS

AFM-techniques proved again to be an important and versatile tool for the elucidation of solid state mechanisms in photochemistry and in gas/solid chemistry. Even though only the surface region of up to several hundred molecular layers is probed in such investigations, it is obvious that we do see the effects of the bulk of the crystals. It is of major importance that extremely well-resolved three-dimensional pictures are obtained and that no details are averaged out. Thus, transport phenomena, minute phase transformations, influences of molecular steps and different mechanisms on different faces of the same crystal are easily detected and this opens up new horizons in solid state chemistry. Also, the important borderline of solid versus liquid state may be looked upon in a different way now, because we have a means at hand to investigate this problem at the level of a few single molecules. The same is true for all crystal defects' discussions which will have to be taken down to the level of unimolecular steps or dislocations in the light of the present experiments. There is no indication that topochemically allowed and running reactions[12] behave principally different from topochemically forbidden reactions. In both cases there are phase transformations with far reaching molecular transports, perhaps with the exclusion of the extremely rare topotactic transformations which have not been studied by AFM yet.

ACKNOWLEDGEMENTS

Thanks are due to Professor Dr. W. Rammensee and Dr. J. Schreuer, Universitaet zu Koeln, for the detection of Miller indices. Furthermore, I am indebted to Dipl. Chem. U. Pogodda and M. Haak for the maintenance of our various computer facilities and to Mrs. E. Reents for technical assistance. Finally I thank L.O.T. GmbH, Darmstadt, for the NanoScope III software and technical advice.

REFERENCES

1. a) G. Kaupp, Angew. Chem. Int. Ed. Engl., 31, 592; 595 (1992); b) GIT Fachz. Labor., 37, 7/93.
2. G. Kaupp, J. Schmeyers, Angew. Chem. Int. Ed. Engl., 32, 1993, in press.
3. G. Kaupp, J. Microscopy, 1993, in press.
4. G. Kaupp, Mol. Cryst. Liq. Cryst., 211, 1 (1992).
5. G. Kaupp, GIT Fachz. Labor., 37, 284 (1993).
6. R. Mason, Acta Cryst., 17, 547 (1964).
7. A. Schmitt, Liebigs Ann. Chem., 127, 319 (1863).
8. J. P. Glusker, D. E. Zacharias, and H. L. Cassell, J. C. S. Perkin II, 1975, 68; M. D. Cohen, Mol. Cryst. Liq. Cryst., 50, 1 (1979).
9. R. E. Buckles, E. A. Hausman, and N. G. Wheeler, J. Am. Chem. Soc., 72, 2494 (1950); R. S. Miller, D. Y. Curtin, and I. C. Paul, ibid., 94, 5117 (1972).
10. G. Kaupp, Mol. Cryst. Liq. Cryst. Inc. Nonlin. Opt., 161, 119 (1988); G. Kaupp, D. Matthies, Chem. Ber., 120, 1897 (1987).
11. J. Bernstein, Acta Cryst., B31, 1268 (1975); J. A. Bouwstra, A. Schouten, and J. Kroon, ibid., C40, 428 (1984).
12. V. Ramamurthy, Tetrahedron, 42, 5753 (1986); G. Kaupp, Handbook of Organic Photochemistry and Photobiology (CRC Press, Inc., Cleveland, 1993), in press.